Practical Approach to MRI of Female Pelvic Masses

Brian C. Allen[1]
Keyanoosh Hosseinzadeh[1]
Shadi A. Qasem[2]
Adam Varner[1]
John R. Leyendecker[1]

OBJECTIVE. Female pelvic masses have a broad differential diagnosis, including benign and malignant neoplasms and nonneoplastic entities.

CONCLUSION. By using a systematic approach to the evaluation of a complex pelvic mass, including incorporating the clinical and surgical history, and by using multiparametric MRI to identify the anatomic origin, morphologic features, and tissue composition of a mass, a short meaningful differential diagnosis or definitive diagnosis can often be established.

Keywords: approach, MRI, pelvic mass, tumor markers

DOI:10.2214/AJR.13.12023

Received October 1, 2013; accepted after revision December 18, 2013.

Presented at the 2013 annual meeting of the ARRS, Washington, DC (exhibit E430, recipient of Bronze Medal award).

[1]Department of Radiology, Wake Forest School of Medicine, Wake Forest Baptist Medical Center, Medical Center Blvd, 3rd Fl MRI, Winston-Salem, NC 27157-1088. Address correspondence to B. C. Allen (bcallen2@wakehealth.edu).

[2]Department of Pathology, Wake Forest School of Medicine, Winston-Salem, NC.

This article is available for credit.

AJR 2014; 202:1366–1375

0361–803X/14/2026–1366

Pelvic masses in female patients have a broad differential diagnosis, including benign and malignant neoplasms and nonneoplastic diseases. Many pelvic masses are a diagnostic challenge, given their proximity to a variety of pelvic structures and the overlap of specific imaging features among different diagnoses. Ultrasound is often the first-line imaging modality for the evaluation of pelvic masses, especially in women, in whom the ovaries are a potential source. However, ultrasound may be limited by poor acoustic windows and poor depth of penetration, preventing characterization of some masses. CT is limited in the pelvis by a lack of soft-tissue contrast, which becomes problematic when, for example, trying to differentiate decompressed bowel from adnexal structures. MRI, on the other hand, provides excellent contrast resolution, resulting in accurate tissue characterization and improved anatomic delineation. As a result, MRI has been shown to be more specific and accurate than ultrasound for characterizing adnexal masses [1, 2]. By using a systematic approach to complex pelvic masses, incorporating the patient's clinical and surgical history, and using MRI to identify the anatomic origin, shape, composition, and enhancement pattern of the mass, a short meaningful differential diagnosis, and often a definitive diagnosis, can be made.

Imaging Protocol

Pelvic MRI is generally performed with a phased-array body coil with the patient supine. A typical pelvic mass protocol begins with a coronal localizer using a fast sequence, such as single-shot turbo or fast spin-echo. This provides an anatomic overview of the lower abdomen and pelvis and, provided an adequately large FOV is selected, allows visualization of the renal collecting systems to assess for hydronephrosis. Axial gradient dual-echo T1-weighted (in- and opposed-phase) imaging is performed with the longer TE assigned to the in-phase echo. In- and opposed-phase imaging allows detection of intravoxel lipid within masses, manifesting as signal loss on the opposed-phase images. The presence of macroscopic lipid within a pelvic mass can be revealed on opposed-phase images by the characteristic India-ink artifact at fat-water interfaces. Gradient dual-echo imaging can also be useful for identifying susceptibility artifacts, which are accentuated on the in-phase images, related to surgical clips, stents, or hemosiderin. Two-point Dixon fat-only and water-only images may be calculated from the gradient dual-echo T1-weighted datasets. These images have improved signal-to-noise ratios compared with dual gradient-echo in- and opposed-phase imaging and may be useful in the identification of small amounts of lipid [3].

Multiplanar high-resolution 2D T2-weighted images without fat suppression provide excellent anatomic detail, delineation of the uterine zonal anatomy, and visualization of the ovarian stroma and follicles. Alternatively, a single 3D T2-weighted sequence can be performed with subsequent postprocessing into any desired plane [4]. Axial fat-sup-

pressed T2-weighted imaging is helpful to identify fluid and edema and may be compared with non-fat-suppressed T2-weighted images to assess for macroscopic lipid. Diffusion-weighted imaging with apparent diffusion coefficient maps has limited utility in characterizing pelvic masses at the present time, but it may be useful for tumor detection and for monitoring response to treatment [5].

Multiphase contrast-enhanced imaging is performed in the desired plane using a 3D fat-suppressed T1-weighted gradient-echo sequence. Unenhanced imaging helps identify hyperintense hemorrhagic or proteinaceous material within lesions and allows subtraction imaging to be performed as an aid to detecting tissue enhancement. Satisfactory data subtraction requires careful breath-holding instructions to ensure that unenhanced and contrast-enhanced images are identically registered. In addition, unenhanced images may be compared with gradient dual-echo T1-weighted images to assess for macroscopic lipid.

TABLE 1: Differential Diagnosis Based on Location of Origin

Origin	Differential Diagnosis
Peritoneal space	Endometriosis, metastasis, primary peritoneal tumor, peritoneal inclusion cyst, abscess
Mesorectal space	Duplication cyst, gastrointestinal stromal tumor, rectal adenocarcinoma, carcinoid, nodal metastasis
Retrorectal and presacral space	Abscess, hematoma, tailgut cyst, epidermoid or dermoid cyst, neurogenic tumor, Tarlov cyst, anterior meningocele, sacrococcygeal teratoma, lymphangioma, myelolipoma
Extraperitoneal space and pelvic sidewall	Abscess, hematoma, aneurysm, lymphangioma, lymphoma, nerve sheath tumor
Ovaries and fallopian tubes	Functional cyst, epithelial neoplasm, sex cord–stromal tumor, germ cell tumor, tuboovarian abscess, hydrosalpinx, ectopic pregnancy, fallopian tube carcinoma, metastasis (Krukenberg tumor)
Round and uterosacral ligaments	Endometriosis, mesothelial cyst, leiomyoma, metastasis, hydrocele of canal of Nuck

Step 1: Determine the Compartment or Organ of Origin

Determining the compartment or organ of origin significantly narrows the differential diagnosis of a pelvic mass. In general, the larger the mass, the more difficult determining the compartment of origin becomes. Fortunately, there are several imaging clues that can help. Because MRI provides excellent soft-tissue contrast resolution and anatomic delineation, it excels in this regard.

Within the pelvis, there are numerous organs, spaces, and potential spaces for which the differential diagnosis will differ (Table 1). Important peritoneal spaces include the vesicouterine and rectouterine recesses. These spaces are best appreciated on sagittal T2-weighted images as the space between the urinary bladder and uterus (vesicouterine) and the rectum and uterus (rectouterine).

Extraperitoneal spaces include the mesorectal, presacral and retrorectal spaces, pelvic sidewalls, and perineum. The mesorectal space is demarcated by the mesorectal fascia, a T2-hypointense structure that envelops the mesorectum and is best seen on axial T2-weighted images. The retrorectal and presacral spaces are demarcated by the posterior rectum and the bony sacrum. The peritoneum along the pelvic sidewalls divide the intraperitoneal space from the iliac vessels, lymph nodes, and connective tissue of the extraperitoneal space. The perineum is located inferior to the pelvic diaphragm, between the pubic symphysis and the coccyx [6].

Tumors can also arise from the urinary bladder, urethra, vagina, uterus, cervix, ovaries, fallopian tubes, and rectum. Masses of the round and uterosacral ligaments are uncommon but do occur.

In female patients, an ovarian origin should always be suspected when confronted with a pelvic mass. Clues to an ovarian origin include a lack of a normal ipsilateral ovary and the presence of follicles surrounding the mass (Fig. 1).

Identifying the blood supply and drainage of a pelvic mass also helps. The presence of an ovarian vascular pedicle, or continuity of the gonadal veins with a pelvic mass, suggests the ovary as the source [7, 8] (Fig. 1). The suspensory ligament, which is a linear or fan-shaped soft-tissue band, attaches the ovary to the pelvic sidewall and contains the ovarian artery and vein. In addition, the ovaries are located anterior or anteromedial to the ureters, so an ovarian mass may displace the ureters posteriorly or posterolaterally [9]. Alternatively, the bridging vascular sign, or identifying bridging vessels between the uterus and a mass, establishes the uterus as the source and leiomyoma as the most likely diagnosis [10, 11] (Fig. 2).

When attempting to place a mass into one of the spaces or potential spaces of the pelvis, it is important to examine how the mass displaces normal anatomic structures (Fig. 3). Displacement of the ipsilateral ureter and iliac vessels medially infers that the mass originates from the extraperitoneal space of the pelvic sidewall. Retrorectal and presacral masses displace the rectum anteriorly or anterolaterally. Intraperitoneal masses, within the rectouterine space, will displace the uterus anteriorly and the rectum posteriorly. Masses within the mesorectal space often arise from the rectum. Superior displacement of the levator ani will place the mass within the perineum.

Step 2: Consider Shape

The shape of a mass can be helpful in establishing the diagnosis (Fig. 4). For example, a peritoneal inclusion cyst tends to surround the ovary and to conform to available space and surrounding structures. Aggressive angiomyxomas are soft tumors that often insinuate between other anatomic structures. Diffuse lymphoma tends to be infiltrative, surrounding vessels without displacing them. Nerve sheath tumors often have an elongated ovoid shape, aligned along a nerve with which it is contiguous. Endometriotic implants often have an irregular border with angulated margin due to fibrosis and adhesions. A potential pitfall involves tubular masses, such as hydrosalpinx, which can appear as a round mass when visualized in only one imaging plane.

Step 3: Analyze Composition

Once the anatomic origin and shape of a mass have been determined, it is important to assess the composition of the mass. MRI excels at tissue characterization, including fluid, hemorrhage, lipid, myxoid tissue, fibrous tissue, smooth muscle, and lymphomatous tissue.

Simple fluid has long T1 and T2 relaxation times and will be hypointense on T1-weighted images and hyperintense on T2-weighted images (Fig. 5). After contrast agent administration, there will be no enhancement of

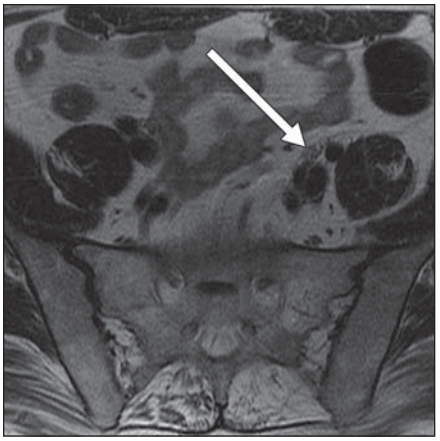

A

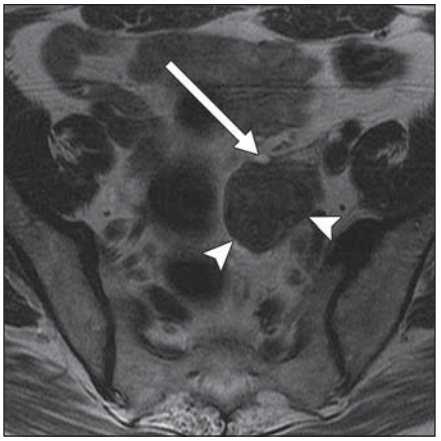

B

Fig. 1—28-year-old woman with left ovarian Brenner tumor.
A and **B,** Axial T2-weighted image (**A**) shows left gonadal vein (*arrow*, **A**) leading to left ovarian mass, as seen in second axial T2-weighted image (**B**), where mass is caudal to **A** and shows follicle (*arrow*, **B**) at periphery of T2-hypointense adnexal mass (*arrowheads*, **B**). Clues to ovarian origin in this case are gonadal vein and peripheral follicle. Absence of normal ipsilateral ovary helped confirm ovarian origin of this mass.

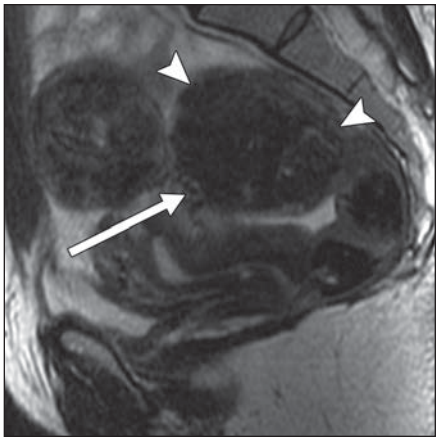

Fig. 2—36-year-old woman with subserosal pedunculated uterine leiomyoma (*arrowheads*), as shown on sagittal T2-weighted MR image. Note vessels and flow voids (*arrow*) between uterus and leiomyoma, which is "bridging vascular sign." Also note T2 hypointensity of leiomyoma, typical of smooth muscle–containing neoplasm.

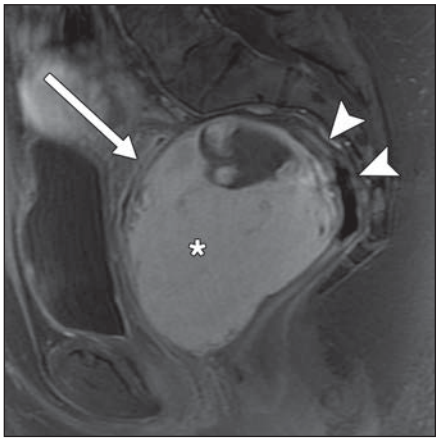

A

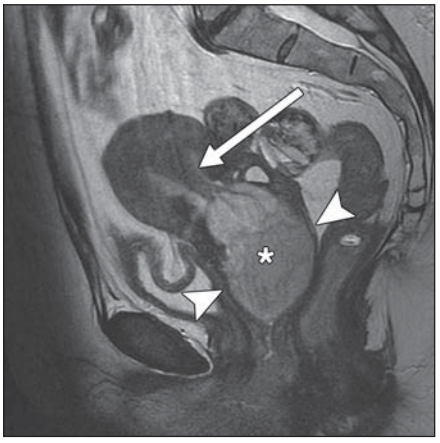

B

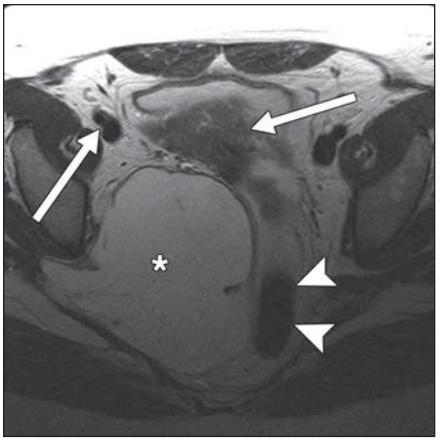

C

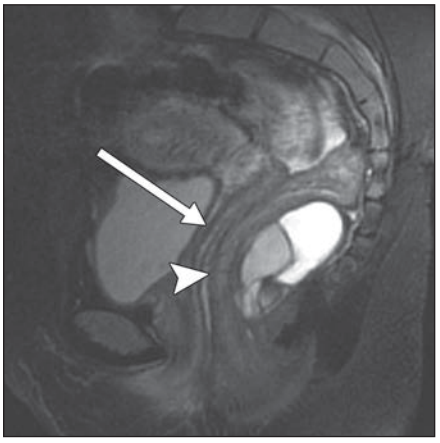

D

Fig. 3—Placing mass into specific location or space will shorten differential diagnosis, as shown for four patients.
A, 29-year-old woman with angiomyofibroblastoma in rectouterine space. Sagittal contrast-enhanced fat-suppressed T1-weighted MR image shows avidly enhancing mass (*asterisk*) in rectouterine space. Mass displaces vagina anteriorly (*arrow*) and rectum posteriorly (*arrowheads*).
B, 43-year-old woman with prolapsing pedunculated leiomyoma distending vagina. Sagittal T2-weighted MR image shows mass (*asterisk*) with vascular stalk (*arrow*) extending from uterus into vagina; anterior and posterior vaginal walls are demarcated by arrowheads.
C, 45-year-old woman with myxoid fibrosarcoma in extraperitoneal space. Axial T2-weighted MR image shows hyperintense mass (*asterisk*) in right pelvic extraperitoneal space extending through greater sciatic foramen into gluteal region. Rectum (*arrowheads*) and mesorectum are displaced laterally, and uterus and iliac vessels (*arrows*) are displaced anteriorly.
D, 22-year-old woman with tailgut cyst. Sagittal T2-weighted MR image shows multilocular cystic mass in presacral space, displacing rectum (*arrowhead*) and vagina (*arrow*) anteriorly.

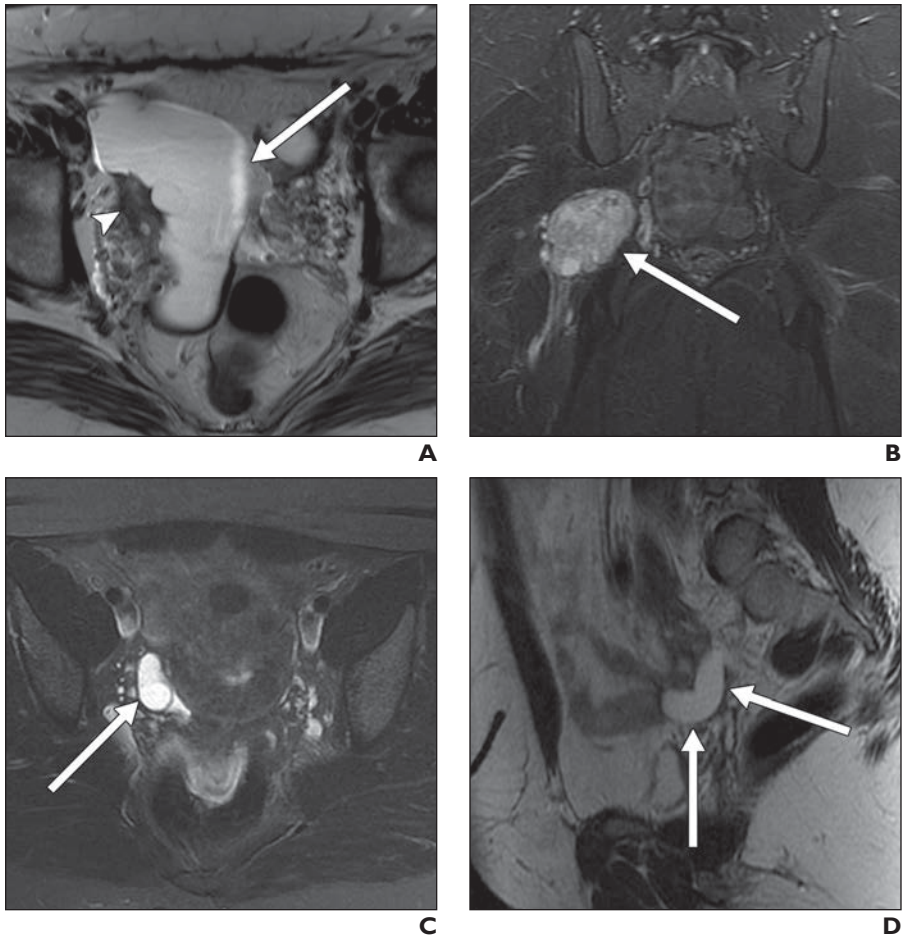

Fig. 4—Shape of mass may be helpful in establishing diagnosis, as shown for three patients.
A, 47-year-old woman with peritoneal inclusion cyst. Axial T2-weighted MR image through pelvis shows hyperintense lesion (*arrow*) in right pelvis. Mass surrounds ovary (*arrowhead*) and conforms to its surroundings.
B, 24-year-old woman with schwannoma. Coronal fat-suppressed T2-weighted image shows elongated, or ovoid-shaped, mass (*arrow*) in extraperitoneal space, contiguous with and oriented with long axis course of sciatic nerve.
C and **D,** 41-year-old woman with right hydrosalpinx. Axial fat-suppressed T2-weighted image (**C**) shows ovoid hyperintense lesion (*arrow*, **C**) in right adnexa. Sagittal T2-weighted image (**D**) shows tubular shape of lesion (*arrows*, **D**).

simple fluid, clearly differentiating simple fluid from myxoid tissue, the latter of which can appear similarly bright on T2-weighted images but enhances [12]. Common cystic masses of the pelvis that can contain simple-appearing fluid include functional ovarian cysts, serous cystadenomas, and peritoneal inclusion cysts (Table 2).

The retrorectal and presacral spaces are other sites where cystic pelvic masses occur. The differential diagnosis of a cystic retrorectal mass includes epidermoid and dermoid cysts, rectal duplication cysts, and anterior meningoceles, all of which are typically unilocular. Multilocular cystic retrorectal masses include tailgut cysts and cystic lymphangiomas [13]. Tailgut cysts, also known as retrorectal cystic hamartomas, are developmental cysts, more frequently found in middle-aged women [14] (Figs. 3D and 5). Depending on the protein content of the cyst fluid, some locules may be hyperintense on T1-weighted images. Tailgut cysts often have thin enhancing septa and can become infected or undergo malignant transformation, altering the imaging appearance [13, 15]. The presence of fat or fat-fluid level in a presacral cystic mass should suggest a dermoid cyst or sacrococcygeal teratoma.

The appearance of blood products is variable on MRI, depending on the age and state of degradation of blood products [16]. In the abdomen and pelvis, methemoglobin and hemosiderin are blood degradation products that are easily imaged with MRI (Table 2). Methemoglobin appears relatively hyper-

TABLE 2: Differential Diagnosis Based on Imaging Characteristics

Composition	Signal Intensity	Common Causes
Simple fluid	T1 hypointense; T2 hyperintense; no enhancement	Functional ovarian cyst, cystic neoplasm, inclusion cyst, hydrosalpinx, tailgut cyst, epidermoid cyst
Blood	T1 hyperintense; T2 variable; no enhancement	Hematoma, hemorrhagic cyst, endometriosis, ectopic pregnancy, hematosalpinx, cystic adenomyosis
Lipid	T1 hyperintense; T2 intermediate; no enhancement	Teratoma, lipoma, liposarcoma, lipoleiomyoma
Myxoid	T1 hypointense; T2 hyperintense; avid enhancement	Angiomyxoma, myxoma, neurogenic tumor, myxoid liposarcoma, myxoid degeneration of leiomyoma
Fibrous tissue	T1 iso- to hypointense; T2 hypointense; mild progressive enhancement	Fibroma, fibrothecoma, Brenner tumor, cystadenofibroma
Smooth muscle	T1 isointense; T2 hypointense; moderate enhancement	Leiomyoma
Lymphoid tissue	T1 isointense; mildly T2 hyperintense; mild homogeneous enhancement	Lymphoma

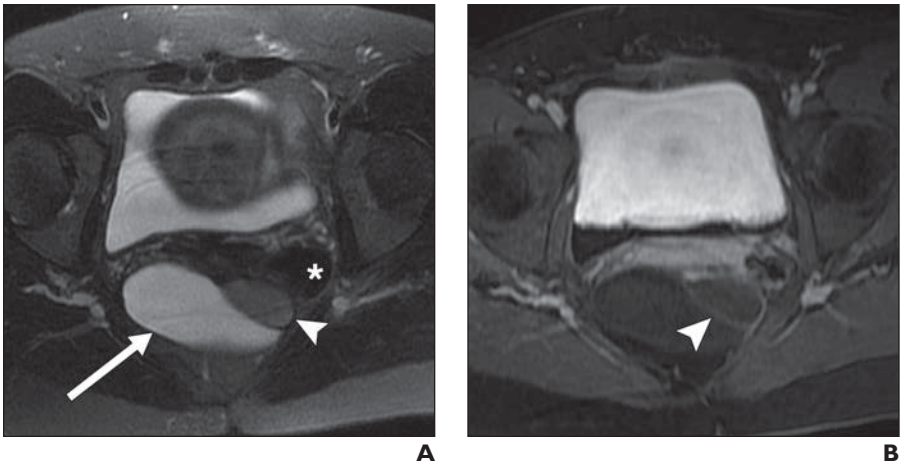

Fig. 5—43-year-old woman with tailgut cyst.
A, Axial fat-suppressed T2-weighted image shows multilocular hyperintense mass (*arrow*) with hypointense component (*arrowhead*), displacing rectum (*asterisk*) anteriorly and to left. T2-hypointense locule likely reflects proteinaceous fluid.
B, Axial contrast-enhanced fat-suppressed T1-weighted MR image shows enhancing septum (*arrowhead*) without internal enhancement of this mass. Combination of T2 hyperintensity and lack of enhancement suggests fluid. Given location and multilocular appearance, diagnosis of tailgut cyst should be considered.

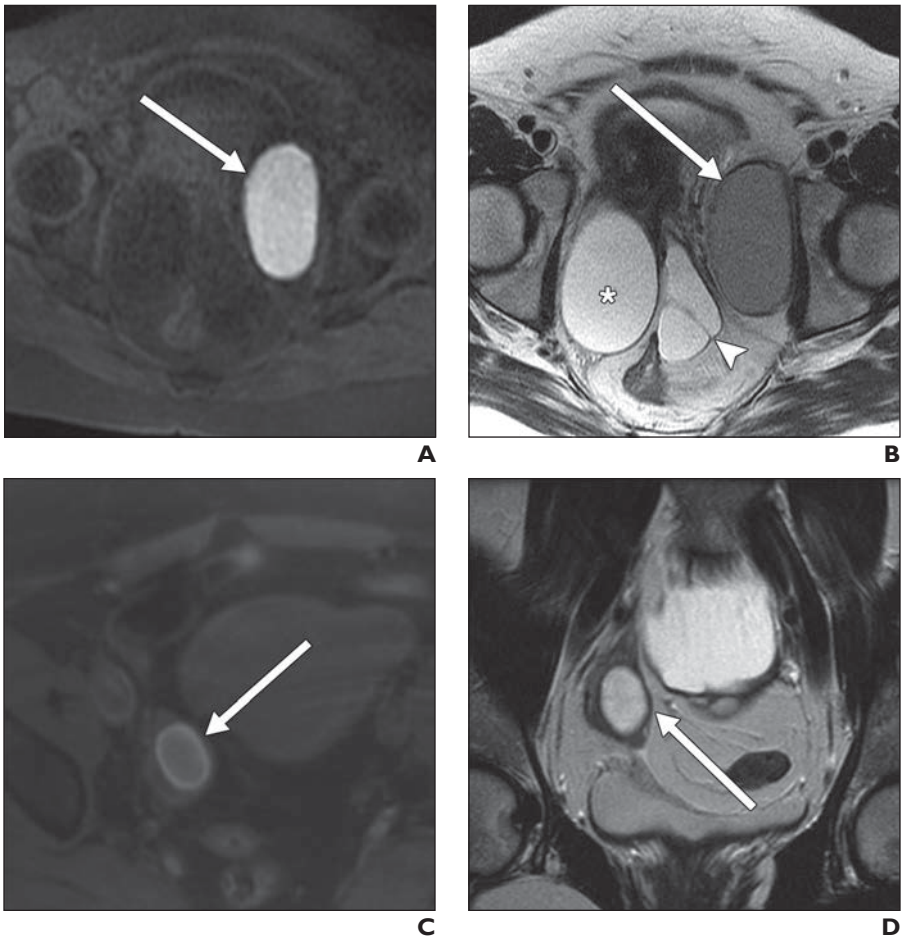

Fig. 6—Two patients with blood-containing pelvic masses.
A and **B,** 36-year-old woman with endometrioma. Axial fat-suppressed T1-weighted MR image (**A**) shows markedly T1-hyperintense left adnexal mass (*arrow*, **A**). Axial T2-weighted MR image (**B**) shows decreased signal intensity within lesion (*arrow*, **B**). T2 appearance of endometriomas relates to recurrent hemorrhage with high iron content causing susceptibility. In addition, there is right adnexal cyst (*asterisk*, **B**) and midline peritoneal inclusion cyst (*arrowhead*, **B**).
C and **D,** 32-year-old woman with hemorrhagic cyst. Axial fat-suppressed T1-weighted MR image (**C**) shows moderately T1-hyperintense right adnexal mass (*arrow*, **C**). Notice that mass is less hyperintense than endometrioma in **A**. Coronal T2-weighted MR image (**D**) shows hyperintensity of this right adnexal mass (*arrow*, **D**).

intense on T1-weighted images and is commonly visible in hematoma, ectopic pregnancy, endometrioma, cystic adenomyosis, hematosalpinx, and ovarian torsion (Fig. 6). Of note, 43% of functional hemorrhagic cysts remain hypointense on T1-weighted sequences as a result of low concentrations of methemoglobin and the presence of preexisting fluid [17]. This contrasts with endometriomas, in which 93% of cysts are hyperintense on fat-suppressed T1-weighted images and are typically of higher signal intensity than hemorrhagic cysts, a finding related to chronic repetitive hemorrhage and higher protein concentration [18]. Because of the recurrent hemorrhage and high iron content within endometriomas, which shortens the T2 relaxation time, endometriomas are typically T2 hypointense [19]. Hemorrhagic endometriotic implants typically contain hyperintense foci on fat-suppressed T1-weighted images surrounded by hypointense desmoplastic tissue. These implants are typically hypointense on T2-weighted sequences [20, 21]. Hemo-

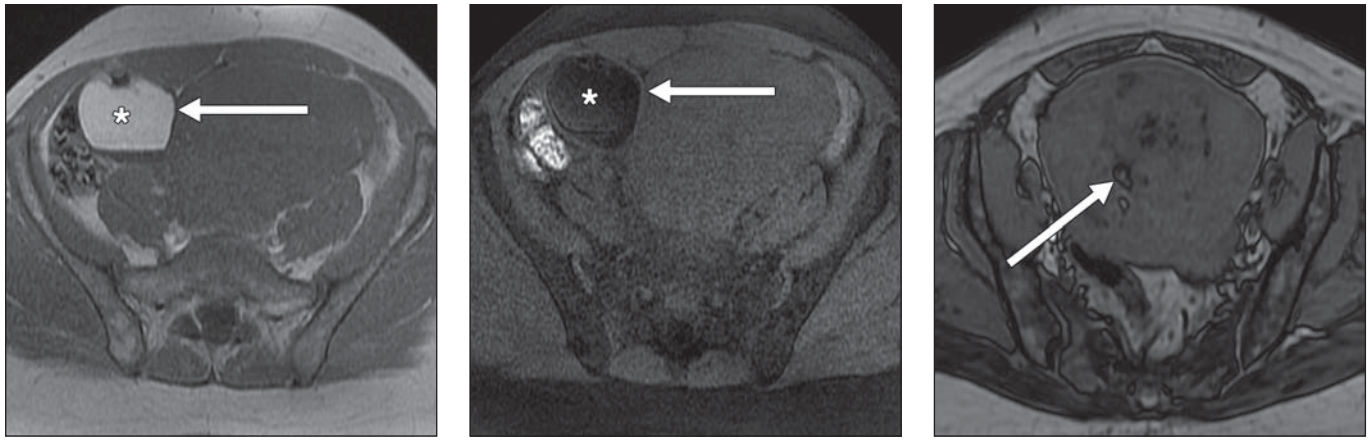

Fig. 7—Two patients with lipid-containing pelvic masses.
A and **B,** 41-year-old woman with right ovarian mature cystic teratoma. Axial in-phase T1-weighted MR image through pelvis (**A**) shows mixed intensity right adnexal mass (*arrow*, **A**). T1-hyperintense portion of this mass (*asterisk*, **A**) represents lipid. On fat-suppressed T1-weighted image (**B**), mass is seen (*arrow*, **B**) but signal loss occurs in T1-hyperintense portion (*asterisk*, **B**).
C, 50-year-old woman with lipoleiomyoma. Axial opposed-phase T1-weighted MR image through pelvis shows India-ink artifact (*arrow*) at lipid and water interfaces.

siderin is hypointense on T1- and T2-weighted images and may be seen as a peripheral rim in mature hematomas or endometriomas [12]. Long-TE gradient-echo imaging improves the conspicuity of hemosiderin.

Lipid is typically hyperintense on non-fat-suppressed T1-weighted images and isointense to subcutaneous adipose tissue on T2-weighted images. On frequency-selective fat-suppressed images, macroscopic lipid signal will be suppressed (Fig. 7). On opposed-phase gradient-echo images, signal loss due to similar amounts of fat and water protons within voxels will be displayed as India-ink artifact at the lipid-water interfaces (Fig. 7). After contrast agent administration, lipid does not enhance [12]. Lipid-containing pelvic tumors include mature cystic teratomas, lipomas and liposarcomas, and lipoleiomyomas (Table 2). Detecting intralesional fat within an adnexal mass suggests the presence of a mature cystic teratoma, commonly referred to as a dermoid cyst. Teratomas are the most common ovarian neoplasm, and most occur in women of reproductive age. Teratomas develop from the three primitive germ cell layers and contain lipid, calcifications, and hair [22]. Lipid-containing uterine tumors include lipomas and lipoleiomyomas [22]. Well-differentiated liposarcomas are the most common retroperitoneal tumors and consist of variable amounts of lipid and soft tissue. Myxoid and pleomorphic liposarcomas typically lack macroscopic lipid [23, 24].

Myxoid tissue is hypointense to isointense on T1-weighted images, hyperintense on T2-weighted images, and shows variable enhancement [12, 25] (Fig. 8). Myxomatous tissue has a very high water content, hence the T2 hyperintensity. Enhancement distinguishes myxoid tissue from fluid [12]. Myxoid-containing tumors include myxomas, aggressive angiomyxomas, neurogenic tumors, myxoid liposarcomas, and myxoid degeneration of leiomyomas (Table 2). Aggressive angiomyxoma is a rare benign neoplasm that arises from the perineum or lower pelvis, typically seen in young women [6, 26–28]. These are soft nonencapsulated tumors that infiltrate the surrounding soft tissues and can recur after excision [27]. Pathologically, aggressive angiomyxomas are gelatinous tumors with a loose myxoid matrix with high water content [27, 29]. Aggressive angiomyxomas avidly enhance after IV contrast agent administration and often have a whorled appearance [28, 30]. Neurogenic tumors such as schwannomas and neurofibromas occur in the extraperitoneal space of the pelvis and are typically round or oval, smaller than 5 cm, and may undergo degenerative changes, such as cyst formation, hemorrhage, and calcification. Myxoid

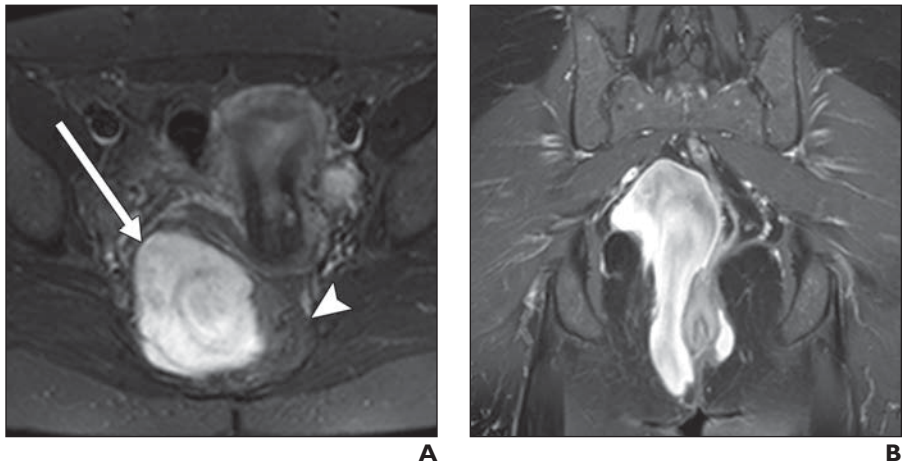

Fig. 8—43-year-old woman with aggressive angiomyxoma.
A, Axial fat-suppressed T2-weighted image shows very hyperintense (near fluid signal) mass (*arrow*) in mesorectal space, displacing rectum (*arrowhead*) leftward.
B, Coronal contrast-enhanced fat-suppressed T1-weighted image shows avidly enhancing mass with "whorled" appearance, invading through pelvic floor. Combination of high T2 signal and avid enhancement, along with insinuating shape of mass, suggest correct diagnosis.

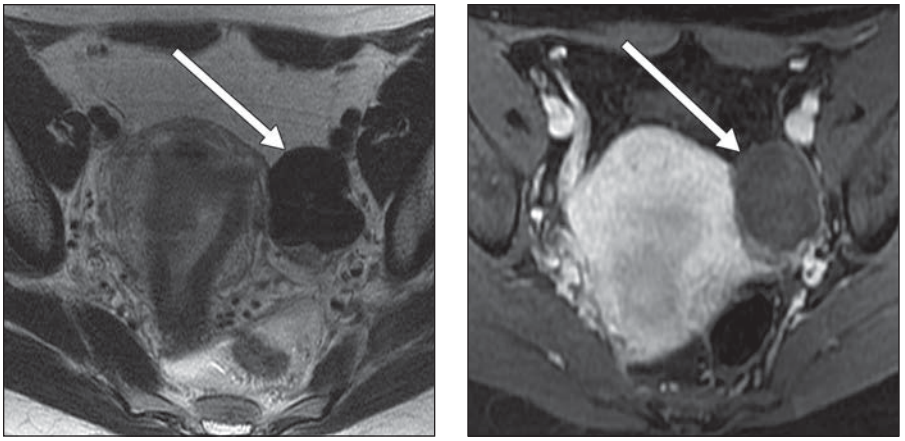

Fig. 9—40-year-old woman with left ovarian fibroma.
A, Axial T2-weighted image shows very hypointense left adnexal mass (*arrow*).
B, Axial contrast-enhanced fat-suppressed T1-weighted image shows hypovascular mass (*arrow*). Combination of very low signal intensity on T2-weighted images and marked hypovascularity suggests densely fibrous tumor, such as fibroma.

elements can occur in schwannomas and, less frequently, in neurofibromas [31]. The target pattern described on T2-weighted imaging for neurogenic lesions is composed of a peripheral high-signal-intensity zone rich in myxoid stroma and a central low-signal-intensity region of high cellularity rich in collagen, a pattern most commonly seen in neurofibromas [32].

Fibrous tissue is typically iso- to hypointense on T1-weighted images, compared with normal myometrium, and hypointense on T2-weighted images, showing slow, progressive, or delayed enhancement [12] (Figs. 1 and 9). Fibrous-containing tumors typically include ovarian neoplasms, such as fibromas and fibrothecomas, Brenner tumors, and cystadenofibromas (Table 2). Fibromas and fibrothecomas are well-defined ovarian stromal tumors that tend to be hypoenhancing, particularly in comparison with normal myometrium and nondegenerated fibroids [33]. They are composed largely of spindle cells in collagenous stroma, which give them their typical hypointense appearance [33]. Cystadenofibromas have both a fibrous component that will appear hypointense on T2-weighted images and an epithelial cystic component, but it is recognition of the T2 hypointense fibrous component that allows one to suggest the diagnosis [34]. Brenner tumors are epithelial-stromal tumors that are often discovered incidentally and can be associated with other epithelial neoplasms. These tumors tend to enhance moderately, but more than fibromas or fibrothecomas [34].

Smooth muscle–containing tumors are T1 isointense, T2 isointense to hypointense to myometrium, and show variable, but often moderate, enhancement [12] (Fig. 2). The prototypical smooth muscle–containing pelvic mass is a nondegenerated uterine leiomyoma (Table 2). Leiomyomas consist of spindle-shaped smooth muscle cells and have a variable amount of collagen and extracellular matrix. On T2-weighted imaging, leiomyomas are well demarcated and are classically of lower signal intensity than normal myometrium [35]. Hyalin degeneration, which commonly complicates leiomyomas, will also be manifest as T2 hypointensity. However, cellular leiomyomas and regions of cystic and myxoid degeneration display as internal T2 hyperintensity. On T1-weighted imaging, leiomyomas approximate the signal intensity of myometrium and usually have

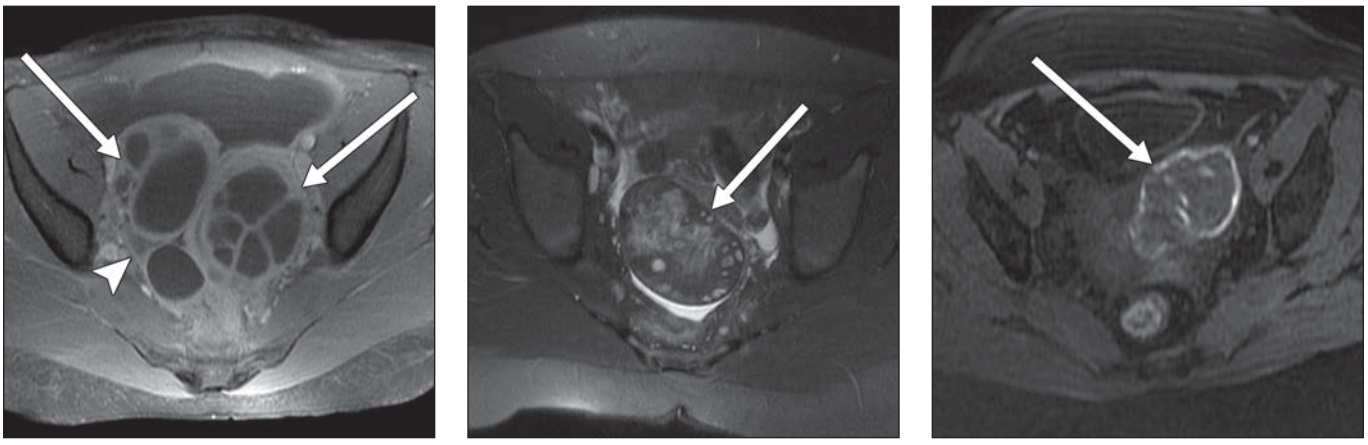

Fig. 10—Clinical and surgical history often allow definitive diagnosis as shown for three patients.
A, 17-year-old girl with tuboovarian abscesses who presented with fever and leukocytosis. Complex multiseptated adnexal masses (*arrows*) with peritoneal thickening and enhancement (*arrowhead*) are seen on axial contrast-enhanced fat-suppressed T1-weighted MR image through pelvis.
B, 10-year-old girl with ovarian torsion who presented with acute right lower quadrant pain. Enlarged edematous right ovary (*arrow*) with surrounding free fluid is seen on axial fat-suppressed T2-weighted MR image through pelvis.
C, 28-year-old woman with ectopic pregnancy who presented with positive pregnancy test but no intrauterine pregnancy. Hemorrhagic left adnexal mass (*arrow*) is seen on axial unenhanced fat-suppressed T1-weighted MR image through pelvis.

TABLE 3: Clinical Questions to Consider When Evaluating Complex Pelvic Masses

Clinical Question	Differential Diagnosis
What is the age and menstrual status of the patient?	Young patients: germ cell neoplasm, sex cord–stromal neoplasm, ectopic pregnancy, tuboovarian abscess. Older patients: ovarian epithelial neoplasm, metastatic disease, sex cord–stromal neoplasm
Are symptoms acute?	Ovarian torsion, ectopic pregnancy, hemorrhagic infarction or torsion of a leiomyoma
Are the symptoms recurrent and cyclic?	Endometriosis
Does the patient have signs and symptoms of infection?	Pelvic inflammatory disease, tuboovarian abscess, hydrosalpinx or pyosalpinx
Has the patient had a prior procedure or prior pelvic inflammation?	Recurrent malignancy, metastatic disease, peritoneal inclusion cyst, endometriosis, postoperative scarring, abscess
Are there predisposing factors for ovarian hyperstimulation, such as ovarian hyperstimulation technique, gestational trophoblastic disease, multiple gestations, or fetal hydrops?	Theca lutein cyst
Does the patient have a known genetic syndrome?	von Hippel–Lindau disease and papillary cystadenoma of the broad ligament; neurofibromatosis and plexiform neurofibroma, solitary neurofibroma or schwannomal; Marfan syndrome and Ehlers-Danlos syndrome and anterior meningocele

variable enhancement after contrast agent administration [36–38].

Lymphoid tissue has a characteristic appearance on MRI. Lymphoma may present as lymphadenopathy, or as an infiltrative soft-tissue mass, and is typically of intermediate signal intensity on T1-weighted images and moderately hyperintense on fat-suppressed T2-weighted images [39]. The characteristic low apparent diffusion coefficient value of lymphoma is thought to relate to the high cellular density of lymphoma with associated diffusivity restriction [40]. After contrast agent administration, expect mild homogeneous enhancement, because necrosis and heterogeneity are not typical features of untreated lymphoma. Rarely, non-Hodgkin lymphoma secondarily involves the ovaries [41–43]. Homogeneous enlargement of the ovaries with these imaging features and peripheral displacement of preserved follicles should suggest the possibility of lymphoma, particularly when associated with adenopathy or extranodal disease elsewhere [39].

Step 4: Put the Mass in Its Clinical Context

Clinical history is extremely important when developing a meaningful differential diagnosis for a complex pelvic mass, and certain questions are important to ask (Table 3). Patient age and presentation are important. If a patient presents with acute pain, the differential diagnosis will be different than if the patient presents with recurrent cyclic pain [44] (Fig. 10). Clinical signs and symptoms, such as fever and leukocytosis, can also help consider a specific diagnosis (Fig. 10). In a female patient of reproductive age, knowing pregnancy status can be critical to excluding or including ectopic pregnancy and theca lutein cysts in the context of bilateral ovarian cystic masses (Fig. 10).

Surgical history is also important to consider. With large pelvic masses, the organ of origin can be difficult to determine. Therefore, it can be helpful to know whether the appendix, uterus, or ovaries have been removed and, if so, for what reason. Also, peritoneal inclusion cysts are seen in women who have undergone pelvic surgery or have had a prior inflammatory process, such as pelvic inflammatory disease (Fig. 4A). Other procedures, if not known at the time of image interpretation, could lead to diagnostic errors. For example, periurethral collagen injected for urinary incontinence may be mistaken for a urethral diverticulum, and mesh plugs from inguinal herniorrhaphy may be mistaken for neoplasm. Certain genetic syndromes may predispose patients to certain neoplasms, including von Hippel–Lindau disease and neurofibromatosis [45, 46] (Table 3).

Laboratory values and tumor markers, if available, may aid in developing a differential diagnosis (Table 4). Several types of ovarian tumors occasionally produce estrogens or androgens [47]. In an adult, estrogen-producing tumors induce endometrial hyperplasia (endometrial thickening) or lead to postmenopausal bleeding. In a premenarchal female, hyperestrogenism results in precocious puberty [48, 49]. Androgens, on the other hand promote the development of male secondary sex characteristics. Hyperandrogenism may lead to hirsutism and virilization with deepening of the voice and increase in muscle mass [48, 49].

Sex cord–stromal tumors include granulosa cell tumors, fibrothecomas, and Sertoli-Leydig cell tumors. Granulosa cell tumors are the most common sex cord–stromal ovarian tumor that leads to hyperestrogenism [49]. Granulosa cell tumors are solid and cys-

TABLE 4: Functioning Ovarian Tumors With Most Common Tumor Markers

Tumor Marker or Abnormal Laboratory Value [Reference]	Differential Diagnosis
β-HCG [49]	Choriocarcinoma, dysgerminoma, ectopic pregnancy
Lactate dehydrogenase [54]	Dysgerminoma, yolk sac tumor
α-Fetoprotein [49, 54]	Yolk sac tumor, embryonal carcinoma, immature teratoma, dysgerminoma
Cancer antigen–125 [53]	Malignant epithelial tumor
Estrogen-producing tumors [49]	Sex cord–stromal tumors (granulosa cell tumor, thecoma or fibrothecoma), steroid cell tumors (stromal luteoma), Epithelial tumors (mucinous cystadenoma, serous cystadenoma)
Androgen-producing tumors [49]	Polycystic ovaries, sex cord–stromal tumors (Sertoli-Leydig cell tumor, stromal luteoma), stromal hyperthecosis, Brenner tumor

tic neoplasms that may contain hemorrhagic fluid in the cystic components. Juvenile granulosa cell tumors are seen in children with precocious puberty as large hemorrhagic multicystic adnexal masses [48]. Thecomas are another sex cord–stromal tumor, typically occurring in postmenopausal women. These are typically solid masses that may occasionally have cystic changes and may lead to hyperestrogenism or hyperandrogenism. On MRI, most thecomas appear as mixtures of fibroma and thecoma and are typically hypointense on T1- and T2-weighted images because of the fibrous tissue [49, 50]. Ovarian fibromas, thecomas, and Brenner tumors are associated with Meigs syndrome, a rare syndrome characterized by ascites, pleural effusion, and a benign ovarian tumor [47].

Germ cell tumors are classified into seminomatous or nonseminomatous tumors [51]. Seminomatous tumors consist of seminomas in the testicles, dysgerminomas in the ovaries, and germinomas in the pineal gland. Nonseminomatous tumors consist of embryonal carcinomas, yolk sac tumors, and choriocarcinomas. Embryonal carcinoma and yolk sac tumors are α-fetoprotein–producing tumors. A small percentage of dysgerminomas (5%) and choriocarcinomas produce β-HCG, which may aid in developing a differential diagnosis [51, 52].

Cancer antigen–125 is widely used for the detection and monitoring of ovarian epithelial carcinoma. However, although cancer antigen–125 is sensitive, with sensitivities reaching approximately 85%, it is not specific for ovarian cancer and is not currently recommended as a screening test [53].

Step 5: Put It All Together

Once the previous four steps have been taken, one need only to look for points of intersection among the lists of entities comprising each category to generate a limited differential diagnosis. In many cases, the list can be reduced to a single final diagnosis. Other features not specifically discussed here, such as multifocality, can also be integrated into the analysis. Even when a final diagnosis is not achievable, providing a limited list of most likely entities can be useful for treatment planning and patient counseling.

Conclusion

Many pelvic masses present a diagnostic challenge. Through excellent contrast resolution, anatomic delineation, and tissue characterization, MRI provides the radiologist with the tools needed to meet this challenge. Although a definite diagnosis is not always possible, a systematic approach to imaging features and clinical context often provides a short meaningful differential diagnosis.

References

1. Bazot M, Darai E, Nassar-Slaba J, Lafont C, Thomassin-Naggara I. Value of magnetic resonance imaging for the diagnosis of ovarian tumors: a review. *J Comput Assist Tomogr* 2008; 32:712–723
2. Sohaib SA, Mills TD, Sahdev A, et al. The role of magnetic resonance imaging and ultrasound in patients with adnexal masses. *Clin Radiol* 2005; 60:340–348
3. Ma J. Breath-hold water and fat imaging using a dual-echo two-point Dixon technique with an efficient and robust phase-correction algorithm. *Magn Reson Med* 2004; 52:415–419
4. Proscia N, Jaffe TA, Neville AM, Wang CL, Dale BM, Merkle EM. MRI of the pelvis in women: 3D versus 2D T2-weighted technique. *AJR* 2010; 195:254–259
5. Namimoto T, Awai K, Nakaura T, Yanaga Y, Hirai T, Yamashita Y. Role of diffusion-weighted imaging in the diagnosis of gynecological diseases. *Eur Radiol* 2009; 19:745–760
6. Hosseinzadeh K, Heller MT, Houshmand G. Imaging of the female perineum in adults. *RadioGraphics* 2012; 32:E129–E168
7. Asayama Y, Yoshimitsu K, Aibe H, et al. MDCT of the gonadal veins in females with large pelvic masses: value in differentiating ovarian versus uterine origin. *AJR* 2006; 186:440–448
8. Lee JH, Jeong YK, Park JK, Hwang JC. "Ovarian vascular pedicle" sign revealing organ of origin of a pelvic mass lesion on helical CT. *AJR* 2003; 181:131–137
9. Saksouk FA, Johnson SC. Recognition of the ovaries and ovarian origin of pelvic masses with CT. *RadioGraphics* 2004; 24(suppl 1):S133–S146
10. Kim JC, Kim SS, Park JY. "Bridging vascular sign" in the MR diagnosis of exophytic uterine leiomyoma. *J Comput Assist Tomogr* 2000; 24:57–60
11. Torashima M, Yamashita Y, Matsuno Y, et al. The value of detection of flow voids between the uterus and the leiomyoma with MRI. *J Magn Reson Imaging* 1998; 8:427–431
12. Siegelman ES, Outwater EK. Tissue characterization in the female pelvis by means of MR imaging. *Radiology* 1999; 212:5–18
13. Yang DM, Park CH, Jin W, et al. Tailgut cyst: MRI evaluation. *AJR* 2005; 184:1519–1523
14. Hjermstad BM, Helwig EB. Tailgut cysts: report of 53 cases. *Am J Clin Pathol* 1988; 89:139–147
15. Aflalo-Hazan V, Rousset P, Mourra N, Lewin M, Azizi L, Hoeffel C. Tailgut cysts: MRI findings. *Eur Radiol* 2008; 18:2586–2593
16. Bradley WG Jr. MR appearance of hemorrhage in the brain. *Radiology* 1993; 189:15–26
17. Kanso HN, Hachem K, Aoun NJ, et al. Variable MR findings in ovarian functional hemorrhagic cysts. *J Magn Reson Imaging* 2006; 24:356–361
18. Togashi K, Nishimura K, Kimura I, et al. Endometrial cysts: diagnosis with MR imaging. *Radiology* 1991; 180:73–78
19. Glastonbury CM. The shading sign. *Radiology* 2002; 224:199–201
20. Siegelman ES, Oliver ER. MR imaging of endometriosis: ten imaging pearls. *RadioGraphics* 2012; 32:1675–1691
21. Coutinho A Jr, Bittencourt LK, Pires CE, et al. MR imaging in deep pelvic endometriosis: a pictorial essay. *RadioGraphics* 2011; 31:549–567
22. Dodd GD 3rd, Budzik RF Jr. Lipomatous tumors of the pelvis in women: spectrum of imaging findings. *AJR* 1990; 155:317–322
23. Craig WD, Fanburg-Smith JC, Henry LR, Guerrero R, Barton JH. Fat-containing lesions of the retroperitoneum: radiologic-pathologic correlation. *RadioGraphics* 2009; 29:261–290
24. Kim T, Murakami T, Oi H, et al. CT and MR imaging of abdominal liposarcoma. *AJR* 1996; 166:829–833
25. Peterson KK, Renfrew DL, Feddersen RM, Buckwalter JA, el-Khoury GY. Magnetic resonance imaging of myxoid containing tumors. *Skeletal Radiol* 1991; 20:245–250
26. Wiser A, Korach J, Gotlieb WH, Fridman E, Apter S, Ben-Baruch G. Importance of accurate preoperative diagnosis in the management of aggressive angiomyxoma: report of three cases and review of the literature. *Abdom Imaging* 2006; 31:383–386
27. Magtibay PM, Salmon Z, Keeney GL, Podratz KC. Aggressive angiomyxoma of the female pelvis and perineum: a case series. *Int J Gynecol Cancer* 2006; 16:396–401
28. Outwater EK, Marchetto BE, Wagner BJ, Siegelman ES. Aggressive angiomyxoma: findings on CT and MR imaging. *AJR* 1999; 172:435–438
29. Fetsch JF, Laskin WB, Lefkowitz M, Kindblom LG, Meis-Kindblom JM. Aggressive angiomyxoma: a clinicopathologic study of 29 female patients. *Cancer* 1996; 78:79–90
30. Jeyadevan NN, Sohaib SA, Thomas JM, Jeyarajah A, Shepherd JH, Fisher C. Imaging features of aggressive angiomyxoma. *Clin Radiol* 2003; 58:157–162
31. Hughes MJ, Thomas JM, Fisher C, Moskovic EC. Imaging features of retroperitoneal and pelvic schwannomas. *Clin Radiol* 2005; 60:886–893
32. Suh JS, Abenoza P, Galloway HR, Everson LI, Griffiths HJ. Peripheral (extracranial) nerve tumors: correlation of MR imaging and histologic

findings. *Radiology* 1992; 183:341–346
33. Shinagare AB, Meylaerts LJ, Laury AR, Mortele KJ. MRI features of ovarian fibroma and fibrothecoma with histopathologic correlation. *AJR* 2012; 198:[web]W296–W303
34. Khashper A, Addley HC, Abourokbah N, Nougaret S, Sala E, Reinhold C. T2-hypointense adnexal lesions: an imaging algorithm. *RadioGraphics* 2012; 32:1047–1064
35. Murase E, Siegelman ES, Outwater EK, Perez-Jaffe LA, Tureck RW. Uterine leiomyomas: histopathologic features, MR imaging findings, differential diagnosis, and treatment. *RadioGraphics* 1999; 19:1179–1197
36. Hamlin DJ, Pettersson H, Fitzsimmons J, Morgan LS. MR imaging of uterine leiomyomas and their complications. *J Comput Assist Tomogr* 1985; 9:902–907
37. Hricak H, Tscholakoff D, Heinrichs L, et al. Uterine leiomyomas: correlation of MR, histopathologic findings, and symptoms. *Radiology* 1986; 158:385–391
38. Ueda H, Togashi K, Konishi I, et al. Unusual appearances of uterine leiomyomas: MR imaging findings and their histopathologic backgrounds. *RadioGraphics* 1999; 19(Spec No):S131–S145
39. Anis M, Irshad A. Imaging of abdominal lymphoma. *Radiol Clin North Am* 2008; 46:265–285 [viii-ix]
40. Punwani S, Taylor SA, Saad ZZ, et al. Diffusion-weighted MRI of lymphoma: prognostic utility and implications for PET/MRI? *Eur J Nucl Med Mol Imaging* 2013; 40:373–385
41. Vang R, Medeiros LJ, Fuller GN, Sarris AH, Deavers M. Non-Hodgkin's lymphoma involving the gynecologic tract: a review of 88 cases. *Adv Anat Pathol* 2001; 8:200–217
42. Monterroso V, Jaffe ES, Merino MJ, Medeiros LJ. Malignant lymphomas involving the ovary: a clinicopathologic analysis of 39 cases. *Am J Surg Pathol* 1993; 17:154–170
43. Osborne BM, Robboy SJ. Lymphomas or leukemia presenting as ovarian tumors: an analysis of 42 cases. *Cancer* 1983; 52:1933–1943
44. Ballard KD, Seaman HE, de Vries CS, Wright JT. Can symptomatology help in the diagnosis of endometriosis? Findings from a national case-control study. Part 1. *BJOG* 2008; 115:1382–1391
45. Choyke PL, Glenn GM, Walther MM, Patronas NJ, Linehan WM, Zbar B. von Hippel–Lindau disease: genetic, clinical, and imaging features. *Radiology* 1995; 194:629–642
46. Patel NB, Stacy GS. Musculoskeletal manifestations of neurofibromatosis type 1. *AJR* 2012; 199:[web]W99–W106
47. Shanbhogue AK, Shanbhogue DK, Prasad SR, Surabhi VR, Fasih N, Menias CO. Clinical syndromes associated with ovarian neoplasms: a comprehensive review. *RadioGraphics* 2010; 30:903–919
48. Outwater EK, Wagner BJ, Mannion C, McLarney JK, Kim B. Sex cord-stromal and steroid cell tumors of the ovary. *RadioGraphics* 1998; 18:1523–1546
49. Tanaka YO, Tsunoda H, Kitagawa Y, Ueno T, Yoshikawa H, Saida Y. Functioning ovarian tumors: direct and indirect findings at MR imaging. *RadioGraphics* 2004; 24(suppl 1):S147–S166
50. Troiano RN, Lazzarini KM, Scoutt LM, Lange RC, Flynn SD, McCarthy S. Fibroma and fibrothecoma of the ovary: MR imaging findings. *Radiology* 1997; 204:795–798
51. Ueno T, Tanaka YO, Nagata M, et al. Spectrum of germ cell tumors: from head to toe. *RadioGraphics* 2004; 24:387–404
52. Zaloudek CJ, Tavassoli FA, Norris HJ. Dysgerminoma with syncytiotrophoblastic giant cells: a histologically and clinically distinctive subtype of dysgerminoma. *Am J Surg Pathol* 1981; 5:361–367
53. Schutter EM, Davelaar EM, van Kamp GJ, Verstraeten RA, Kenemans P, Verheijen RH. The differential diagnostic potential of a panel of tumor markers (CA 125, CA 15-3, and CA 72-4 antigens) in patients with a pelvic mass. *Am J Obstet Gynecol* 2002; 187:385–392
54. Kawai M, Kano T, Kikkawa F, et al. Seven tumor markers in benign and malignant germ cell tumors of the ovary. *Gynecol Oncol* 1992; 45:248–253

FOR YOUR INFORMATION

This article is available for CME and Self-Assessment (SA-CME) credit that satisfies Part II requirements for maintenance of certification (MOC). To access the examination for this article, follow the prompts associated with the online version of the article.